ISSN 1063-7826, Semiconductors, 2016, Vol. 50, No. 1, pp. 89–96. © Pleiades Publishing, Ltd., 2016.
Original Russian Text © E.A. Levchuk, L.F. Makarenko, 2016, published in Fizika i Tekhnika Poluprovodnikov, 2016, Vol. 50, No. 1, pp. 89–96.

SEMICONDUCTOR STRUCTURES, LOW-DIMENSIONAL SYSTEMS, AND QUANTUM PHENOMENA

On Controlling the Electronic States of Shallow Donors Using a Finite-Size Metal Gate

E. A. Levchuk* and L. F. Makarenko

Belarusian State University, ul. F. Skorina 4, Minsk, 220050 Belarus

** e-mail: liauchuk@bsu.by*

Submitted January 12, 2015; accepted for publication May 13, 2015

Abstract—The effect of an external electric field on the states of a shallow donor near a semiconductor surface is numerically simulated. A disk-shaped metal gate is considered as an electric-field source. The wavefunctions and energies of bound states are determined by the finite-element method. The critical characteristics of electron relocation between the donor and gate are determined for various gate diameters and boundary conditions, taking into account dielectric mismatch. The empirical dependences of these characteristics on the geometrical parameters and semiconductor properties are obtained. A simple trial function is proposed, which can be used to calculate the critical parameters using the Ritz variational method.

DOI: 10.1134/S1063782616010127

1. INTRODUCTION

The physical implementation of quantum calculations based on phosphorus-doped silicon, proposed in [1], stimulated the publication of a number of papers in which the effect of an external electric field on donor states near a semiconductor surface was theoretically studied (see [2–9]). In these papers, emphasis was placed on controlling the donor electron density using an external electric field, when the calculated parameter of the given systems was the critical field [5, 6] or the critical gate potential Φ_{0C} [2] corresponding to the donor electron wavefunction shuttling to the gate region. Another calculated parameter important for controlling the electron density is the minimum energy gap ($g_{\min}$) between the ground and first excited electronic states. The quantity $g_{\min}$ allows estimation of the electron-tunneling time from the donor to the gate [5, 6, 10].

The values of Φ_{0C} and $g_{\min}$ depend on a number of geometrical parameters of the system: the donor–semiconductor boundary distance z_0, the gate diameter d; and semiconductor properties: the permittivity ε_s, the effective electron mass m^*, and others. Some of these dependences were studied in [2–8], where different specific cases of sets of these parameters were considered.

For example, in [2], the effect of the donor position and gate sizes on the characteristics of wavefunction control was studied. In [3] a similar problem but for another geometrical configuration of the gate and other boundary conditions for the controlling external field was solved. In later studies [4–7], the gate area was considered to be infinitely large, which provided a uniform electric field in the gate region. In [4–8], unlike [2, 3], the potentials of donor and electron images were additionally considered in the calculation. Thus, in different studies, the models of the structure under study had significant differences in the set of considered factors, which complicates quantitative comparison of the results of different works and does not allow consistent tracing of the effect of some model parameters on the behavior of donor wavefunctions, the critical potential, and the energy gap.

The objective of this work is to study the effect of the geometrical parameters of a metal–semiconductor structure (gate sizes, types of boundary conditions for the electric potential and image potential) and the donor position on the wavefunction shuttling of a donor-bound electron. The electron wavefunctions and energy levels in the gate–donor system were calculated using the finite-element method (FEM) which has a number of advantages over the conventional Ritz method; furthermore, at present, it can be rather easily implemented using available mathematical software packages (see, e.g., MATLAB [11]).

2. PROBLEM STATEMENT

In the present paper, as in [2], we consider a disk-shaped gate of diameter d. The region $z > 0$ is filled with a semiconductor with the permittivity ε_s, and the gate is in the $z = 0$ plane. The donor lies on the gate axis at a distance of z_0 from the gate. It is assumed that an insulator with infinitesimal thickness ($t_{ox} \to 0$) is between the gate and semiconductor. This insulating

layer does not affect the potential distribution, but prevents electron escape from the semiconductor. In this case, an infinitely high potential barrier at the semiconductor boundary is assumed.

In the $z = 0$ plane, two types of boundary conditions for the electric potential induced by the gate were considered. In the first case, it was supposed that the region $z < 0$ is filled with the insulator, the gate thickness was assumed to be infinitesimal (case BC-A). Such a system was previously considered in [2]. In the second case, in the boundary region $z = 0$, $\rho > d/2$, the electric-field potential was set to zero, i.e., it was thought that the gate is surrounded by a grounded metal screen (case BC-B). Such boundary conditions were previously used in [3]. In both cases, the gate potential is denoted by Φ_0.

The electronic states were considered in the approximation of the effective mass which was considered to be isotropic. Although a number of previous papers considered shallow donors in silicon which has an anisotropic effective mass and complex structure of the conduction band, in our opinion, it is reasonable to first consider the isotropic case in more detail; the effect of band-structure features can be considered later, after revealing the main features caused by the spatial characteristics of an external field.

The Schrödinger equation for the wavefunction ψ and electron energy E for σ-states with cylindrical symmetry, in the general case, in the presence of a donor center near the boundary, is written as

$$(\hat{T} + \hat{V}_G^{(i)} + \hat{V}_D + \hat{V}_{D'} + \hat{V}_{im})\psi = E\psi, \ \rho > 0 \ z > 0, \quad (1)$$

where (ρ, z) are cylindrical coordinates. The Hamiltonian includes the following terms: $\hat{T}$ is the kinetic-energy operator,

$$\hat{T} = -\frac{1}{\rho}\frac{\partial}{\partial\rho}\left(\rho\frac{\partial}{\partial\rho}\right) - \frac{\partial^2}{\partial z^2}, \quad (2)$$

$\hat{V}_D$ is the potential energy of the electron–donor interaction:

$$\hat{V}_D = -\frac{2}{\sqrt{(z - z_0)^2 + \rho^2}}, \quad (3)$$

$\hat{V}_{D'}$ is the potential energy of the electron–donor image interaction, $\hat{V}_{im}$ is the potential energy of the electron interaction with its image, $\hat{V}_G^{(i)}$ is the electron potential energy in an external field with i = A, B for the cases BC-A and BC-B, respectively. Analytical expressions for $\hat{V}_G^{(i)}$ are given in [12, 13] (see also Appendix).

Since the electron cannot penetrate the region $z < 0$, the boundary condition

$$\psi|_{z=0} = 0, \ \rho > 0 \quad (4)$$

should be satisfied. For bound states, the conditions

$$\psi \xrightarrow[\rho\to\infty]{} 0, \ \psi \xrightarrow[z\to\infty]{} 0 \quad (5)$$

should also be satisfied.

Equation (1) is presented in the dimensionless form: the effective Bohr radius was used as a distance measuring unit,

$$a^* = \frac{4\pi\varepsilon_0\varepsilon_s\hbar^2}{m^*e^2}, \quad (6)$$

the energy measure is the effective Rydberg

$$Ry^* = \frac{\hbar^2}{2m^*(a^*)^2} = \frac{1}{4\pi\varepsilon_0\varepsilon_s}\frac{e^2}{2a^*}, \quad (7)$$

where m^* is the electron effective mass. Accordingly, the potential was measured in Ry^*/e.

3. CALCULATION RESULTS

3.1. Bound Electron States in the Gate Field for the Case of an Infinitely Distant Donor

Let us first consider a specific case of the problem (1), (4)–(5) in which the electron moves only in the attracting gate field and the donor with which the electron is bound is infinitely distant from the gate. Then the effect of the donor electric potential can be neglected, and the potential well near the gate can be considered as an electrically induced quantum dot; therefore, this problem is of independent interest [9].

Let us first consider the problem with an infinitely distant donor without regard to the effect of the image potential. Then only one potential energy operator $\hat{V}_G^{(i)}$ remains in Eq. (1), which in both cases of BC-A and BC-B represents the expression $\hat{V}_G^{(i)} = \Phi_0 g(d, \rho, z)$, where the function g is homogeneous with respect to d, ρ, z, i.e., $g(d, \rho, z) = g(1, \rho/d, z/d)$ (see Appendix). Therefore, it is natural to choose d and $Ry^*_\delta = Ry^*/\delta^2$ (where $\delta = d/a^*$) as the length and energy units. Accordingly, the gate potential will be expressed in units of Ry^*_δ/e. As a result, we obtain the equation

$$(\hat{T} + \hat{V}_G^{(i)})\psi(\rho, z) = E\psi(\rho, z), \ \rho > 0, \ z > 0, \quad (8)$$

which is invariant with respect to the gate diameter.

We denote the gate potential given in units of Ry^*_δ/e and the ground-state energy expressed in Ry^*_δ as $\tilde{\Phi}_0$ and $\tilde{E}_0$, respectively.

The problem (8) with boundary conditions (4), (5) was solved using the finite-element method (FEM). In this case, the halfspace $\rho > 0$, $z > 0$, in which the problem is defined, was replaced with the bounded region $0 < \rho < L_p$, $0 < z < L_z$, and the wavefunction was approximated using piecewise linear trial functions on a triangular grid. The errors of the determined energies

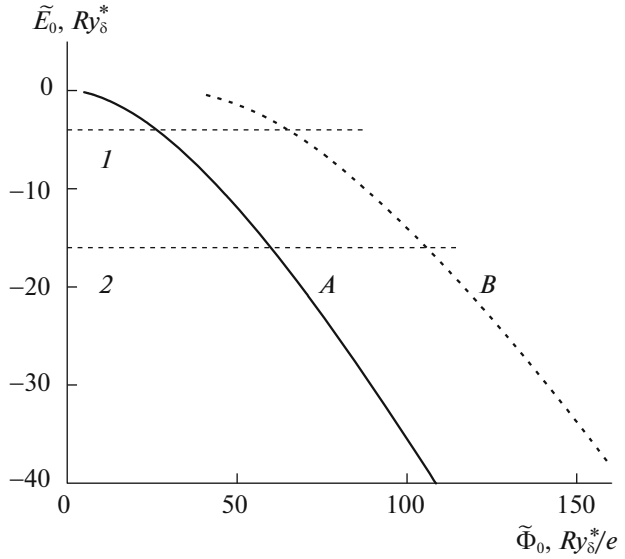

Fig. 1. Dependence of the electron ground-state energy in the gate field on the gate potential. The gate diameter and $Ry^*_\delta = Ry^*/\delta^2$ are used as the length and energy units, respectively. Curves *A* and *B* correspond to boundary conditions BC-A and BC-B, respectively. Straight lines *1* and *2* correspond to $\tilde{E}_0 = -\delta^2 Ry^*_\delta$, where $\delta = 2(d = 2a^*)$ and $\delta = 4(d = 4a^*)$.

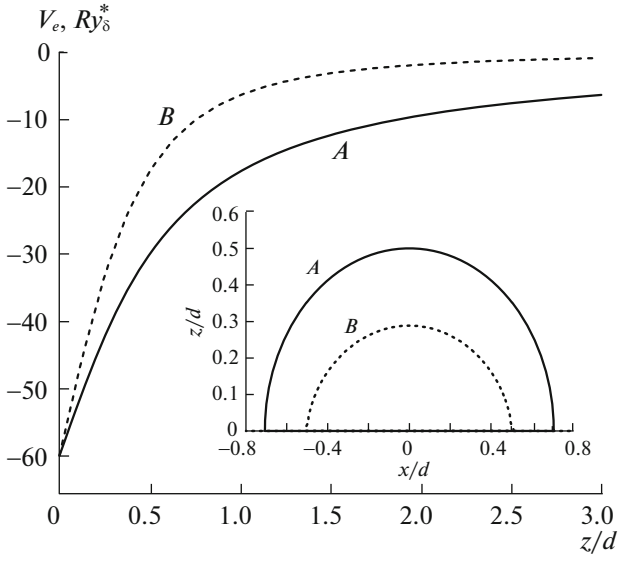

Fig. 2. Electron potential energy in the gate field for a cross section along the $\rho = 0$ axis. The inset shows isolines for the electron potential energy $V_e = -30Ry^*_\delta$ in the gate field. The gate potential is $\tilde{\Phi}_0 = 60Ry^*_\delta$. Curves *A* and *B* correspond to boundary conditions BC-A and BC-B, respectively.

depend on both the choice of L_p and L_z and the grid size. Therefore, in the case of a limited number of nodes, the error in determining the ground-state energy E_0 will first decrease and then increase with increasing L_p and L_z. For this reason, in calculating the ground-state energies, the values of L_p and L_z were chosen from the condition of E_0 minimum.

The dependences $\tilde{E}_0(\tilde{\Phi}_0)$ in the cases of BC-A and BC-B, obtained using the FEM, are shown in Fig. 1. We can see the effect of the boundary conditions for the electric potential on $\tilde{E}_0$: in the case of BC-B, significantly higher external-field potentials are required to provide the same ground-state energy as in the case of BC-A. This is caused by the fact that the external-field potential decreases more rapidly with increasing distances to the gate in the case of BC-B, than in the case of BC-A (Fig. 2). Therefore, the region of electric-field localization in the case of BC-B is smaller (see the inset in Fig. 2). As a result, the region of wavefunction localization is also smaller, which leads to an increase in the contribution of the electron kinetic energy.

The obtained dependences $\tilde{E}_0(\tilde{\Phi}_0)$ allows estimation of the critical potential for various gate diameters at long donor–semiconductor-surface distances ($z_0 \to \infty$). Ground-state wavefunction shuttling from the donor to the gate occurs, when the electron energy level in the gate potential well (curves *A* and *B* in Fig. 1) is lower than its energy in the donor potential well, equal to $-1Ry^*$. Thus, the critical potential can be determined from Fig. 1 by the intersection points of curves $\tilde{E}_0(\tilde{\Phi}_0)$ with straight lines $E_0 = -1Ry^* = -\delta^2 Ry^*_\delta$ (lines *1* and *2* in Fig. 1).

For gate diameters larger than $6a^*$, the dependences $\tilde{E}_0(\tilde{\Phi}_0)$ allow simple empirical approximation using the power function

$$\tilde{E}_0(\tilde{\Phi}_0) \approx -0.0802(\tilde{\Phi}_0)^{4/3} \quad (9)$$

in the case of BC-A and

$$\tilde{E}_0(\tilde{\Phi}_0) \approx -0.00833(\tilde{\Phi}_0)^{5/3} \quad (10)$$

in the case of BC-B. Then at $z_0 \to \infty$ and $d \geqslant 6a^*$, the critical potential can be approximated by the expression

$$\Phi_{0C} \approx c\delta^{-\tau}, \quad (11)$$

where $c = 6.63$, $\tau = 1/2$ for the boundary conditions of BC-A and $c = 17.7$, $\tau = 4/5$ for the boundary conditions of BC-B.

The use of units of d and Ry^*_δ in Eq. (8) makes it possible to represent the electron wavefunctions in the gate field ψ_G (curves *1*–*3* in Fig. 3) in a universal form independent of the gate diameter. At the same time, the shape of the wavefunctions of the hydrogenlike donor, described by the expression $\psi_D = \exp(-r/a^*)$ (curves *1'*–*3'* in Fig. 3) varies for different gate diam-

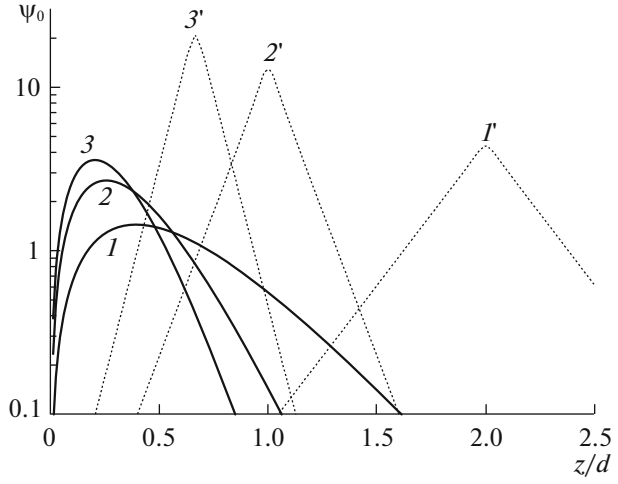

Fig. 3. Normalized ground-state wavefunctions for a cross section along the $\rho = 0$ axis. Curves *1–3* are the gate-state wavefunctions at $\tilde{\Phi}_0 = 60Ry^*_\delta$, $\tilde{\Phi}_0 = 150Ry^*_\delta$, and $\tilde{\Phi}_0 = 260Ry^*_\delta$, which are equal to approximate values of the critical potential for $d = 4a^*$, $d = 8a^*$, and $d = 12a^*$. Curves *1'–3'* are the ground-state wavefunctions of a donor-bound electron in the absence of external field at $z_0 = 8a^*$. For functions *1,1'*, *2,2'*, *3,3'*, $d = 4a^*$, $8a^*$, $12a^*$, respectively.

eters, which appears for different degrees of ψ_G and ψ_D overlap for different values of d at the same donor position ($z_0 = \text{const}$).

To qualitatively study the behavior of the electron wavefunction, it is preferred that the variational method with a small basis be used. The variational method in this form makes it possible to significantly decrease the computational cost and to obtain a clear physical interpretation of the calculated results. In this case, the main problem lies in optimal choice of the trial function. To describe the gate states, functions containing Gaussians [2] or a combination of exponential functions and a Gaussian [5, 6] were previously used. In this case, the variational parameters can enter the trial functions both nonlinearly (e.g., in [5, 6], where they appeared in the exponents and Gaussians) and linearly. The latter version of the trial function construction was used in [2], where gate states were approximated using a linear combination of 25 basis functions. We found that a good approximation for solving the problem (8), (4)–(5) in the case of BC-A is the trial function

$$\psi_G(\rho, z) = N_G z(e^{-\alpha_1\rho^2-\beta_1 z^2} + C_r e^{-\alpha_2\rho^2-\beta_2 z^2}) \qquad (12)$$

with variational parameters α_1, β_1, α_2, β_2, and C_r varying depending on the gate potential $\tilde{\Phi}_0$. The factor z provides fulfillment of boundary condition (4); N_G is the normalization constant.

The parameters α_1, β_1, α_2, β_2 were chosen from the condition of ground-state-energy minimization using the Nelder–Mead method. When $\tilde{\Phi}_0$ is in the range from 30 to 320, the dependences of α_1, β_1, β_2 on the gate potential are well approximated by linear functions. For arbitrary gate diameters, these dependences are written as

$$\alpha_1 = \beta_1 = -0.266/\delta^2 + 0.0275\Phi_0, \qquad (13)$$

$$\beta_2 = 0.256/\delta^2 + 0.0731\Phi_0. \qquad (14)$$

Parameter α_2 can be approximated as

$$\alpha_2 = (0.8 - 0.00172\Phi_0\delta^2)\cdot\beta_2. \qquad (15)$$

In the case of such an approximation of the parameters α_1, β_1, α_2, β_2, the coefficient C_r in function (12) is expressed as

$$C_r = \begin{cases} 2, & 30/\delta^2 < \Phi_0 < 80/\delta^2 \\ 2.33 - 0.00442\Phi_0\delta^2, & \Phi_0 \geq 80/\delta^2. \end{cases} \qquad (16)$$

The quality of trial function (12) with parameters (13)–(15) was estimated by comparing the ground-state energies obtained by the variational method with corresponding values calculated by the FEM. The relative difference between the energies was no more than 1%, which is quite acceptable for further use in the model under consideration.

Let us now estimate the effect of image charges on the ground-state energy. For an infinitely distant donor, it will be only the energy of the electron interaction with its image, which, in the dimensionless form, is given by (see, e.g., [5, 6, 8])

$$\hat{V}_{im} = \frac{Q^*}{2z}. \qquad (17)$$

Equation (17) is written using the dimensionless parameters a^* for length and Ry^* for energy. The factor Q^* is defined by the permittivities of the two adjacent media,

$$Q^* = \frac{\varepsilon_s - \varepsilon_{ins}}{\varepsilon_s + \varepsilon_{ins}},$$

where ε_{ins} is the medium permittivity in the region $z < 0$. For the metal–semiconductor interface, we have $\varepsilon_{ins} \to +\infty$ and $Q^* = -1$.

As seen from Eqs. (1) and (17), if we choose the gate diameter as the length unit, we obtain $\tilde{\hat{V}}_{im} = \delta\hat{V}_{im}$. Therefore, in calculating the effect of the image potential, we used the initial dimensionless parameters a^* and Ry^* instead of d and Ry^*_δ. In this case, the dependences of E_0 on Φ_0 for different gate diameters will differ (see curves *B1* and *B2* in Fig. 4). These depen-

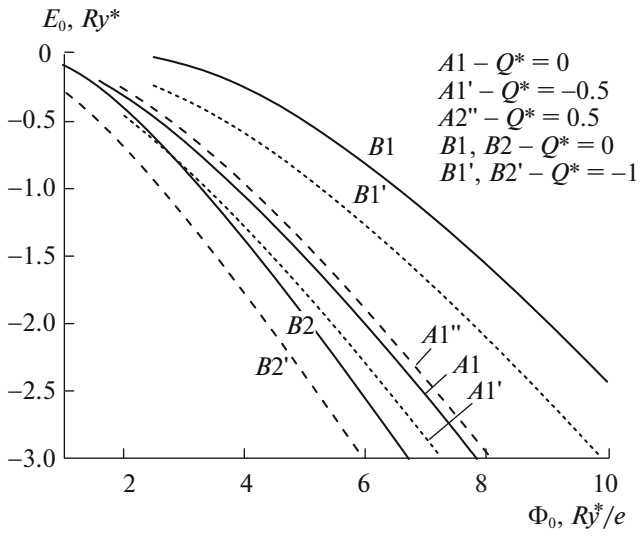

Fig. 4. Electron ground-state energy in the gate field as a function of Φ_0 in units of Ry^*. Curves *A1*, *A1'*, *A1"* correspond to the case of boundary conditions BC-A with $d = 4a^*$, curves *B1*, *B2*, *B1'*, *B2'* correspond to the case of boundary conditions BC-B. The gate diameter is $d = 4a^*$ for *B1*, *B1'* and $d = 8a^*$ for *B2*, *B2'*.

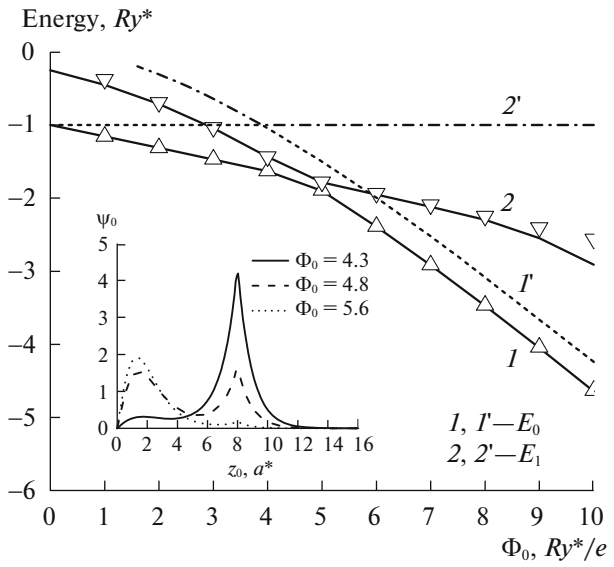

Fig. 5. Dependences of the energies of the ground and first-excited states on the gate potential for boundary conditions BC-A for an infinitely distant donor (curves *1'*, *2'*) and for $z_0 = 8a^*$ (curves *1*, *2*); $d = 4a^*$. The inset shows the normalized functions of the ground state for various gate potentials, $d = 4a^*$, $z_0 = 8a^*$, boundary conditions BC-A.

dences are recalculated from the data shown in Fig. 1 by the formula

$$E_0(\Phi_0) = \tilde{E}_0(\delta^2\tilde{\Phi}_0)/\delta^2. \quad (18)$$

In the numerical simulation in the case of BC-A, as a semiconductor, we choose silicon with $\varepsilon_s = 11.4$ and consider two choices of insulator. In the first case, the insulator is silicon dioxide with $\varepsilon_{ins} = 3.8$ and $Q^* = 0.5$; in the second case, it is an insulator with $\varepsilon_{ins} = 3\varepsilon_s$ and $Q^* = -0.5$ (an example of an insulator with high permittivity can be hafnium dioxide [14]). In the case of BC-B, only the case $Q^* = -1$ (semiconductor–metal interface) takes place. The calculation results are shown in Fig. 4.

As follows from these data, consideration of the image potential does not qualitatively change the behavior of the dependence $E_0(\Phi_0)$, although the relative contribution of the image at small Φ_0 can be rather high (the ground-state energies can differ by an order of magnitude). At large Φ_0, the relative energy change is not so significant (tens of percent). Since consideration of the image does not lead to qualitative changes, in what follows, the image potential can be considered as some correction, and all calculations can be performed assuming $\hat{V}_{D'} = 0$ and $\hat{V}_{im} = 0$.

For an infinitely distant donor, the second critical parameter $g_{\min}$ is zero. As shown in [10], this parameter is related to the probability of tunneling between two potential wells (donor and gate). In this case, it is clear that this probability tends to zero. With decreasing donor–gate distance, $g_{\min}$ will increase. The dependence of $g_{\min}(z_0)$ is studied in the next section.

3.2. Electron States in the Donor–Gate System at a Finite Donor–Gate Distance

In contrast to the case of an infinitely distant donor, where potential wells can be considered isolated from each other, at finite z_0 the electron is simultaneously affected by the donor and gate potentials, which results in a decrease in the stationary state energy. This difference is illustrated in Fig. 5 showing the ground- (E_0) and first-excited- (E_1) state energies calculated by the FEM for $z_0 \to \infty$ and $z_0 = 8a^*$. The additional contribution of the gate potential results in a gradual decrease in the donor-bound electron energy with increasing Φ_0, whereas the isolated donor energy at $z_0 \to \infty$ remains unchanged with increasing Φ_0. The difference in the subgate-state energies for the cases $z_0 \to \infty$ and a finite value of z_0 is almost independent of the gate potential, since the contribution of the donor potential to the total electron potential energy near the gate remains unchanged.

At $z_0 \to \infty$, the dependences of E_0 and E_1 have a common point ($g_{\min} = 0$), by whose position the critical potential is determined. For finite values of z_0, the phenomenon of energy-level anticrossing [15] is observed as Φ_0 increases (Fig. 5), and the critical potential is determined by determining the minimum of the difference $E_1 - E_0$ (see [6]). At $\Phi_0 < \Phi_{0C}$, the

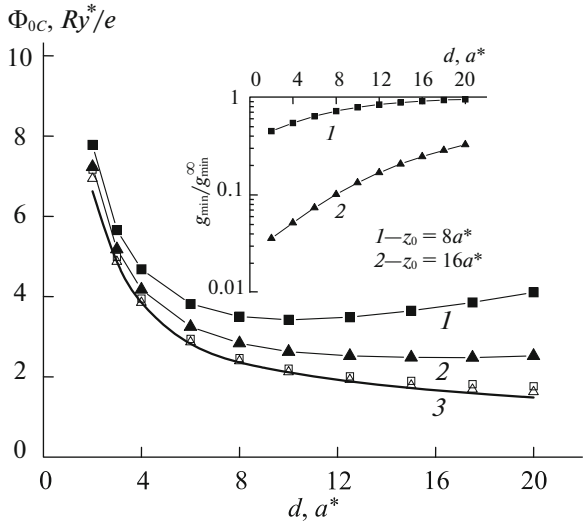

Fig. 6. Dependence of the critical potential on the gate diameter in the case where the region $z < 0$ is filled with an insulator. Curve *1* was determined using formula (11) and Fig. 1, curves *2* and *3* were constructed as the least difference $E_1 - E_0$. Open triangles and squares are the critical potential differences for $z_0 = 16a^*$ and $z_0 = 8a^*$, respectively. The inset shows the dependence of the ratio of the energy gap for a finite gate diameter to the gap for a uniform field on the gate diameter.

probability of finding the electron near the donor is higher than near the gate; at $\Phi_0 > \Phi_{0C}$, gradual electron shuttling to the gate occurs (see the inset in Fig. 5).

In addition to determination of the minimum difference $E_1 - E_0$, one more method for calculating Φ_{0C} is the variational method with a trial function representing the linear combination of two functions:

$$\psi_\Sigma = C_G\psi_G + C_D\psi_D, \qquad (19)$$

where ψ_G and ψ_D are the ground-state wavefunctions in the gate and donor potential wells, respectively. Then the critical potential corresponds to the point at which $C_G = C_D$.

For calculations in the case of BC-A and without regard to the image potential ($\hat{V}_{D'} = 0$, $\hat{V}_{im} = 0$), function (12) with parameters (13)–(16) was used as ψ_G in (19). The function ψ_D was set equal to $N_D\exp(-\alpha\sqrt{(z-z_0)^2+\rho^2})$, where N_D is the normalization factor and α is the variational parameter. Numerical experiments showed that variation in parameter α does not result in a significant decrease in the energy-calculation error; therefore, in what follows, $\alpha = 1$ was used.

The results of calculations of the ground- and first-excited-state energies using trial function (19) are shown in Fig. 5 (triangles). Comparison with the values obtained by the FEM (curves) shows that trial function (19) gives a good approximation for E_0 and E_1 at relatively low gate potentials. At the same time, the trial function at higher Φ_0 is inapplicable in the determination of E_1. As follows from the FEM calculations, at such Φ_0, additional local extrema appear outside the symmetry axis in the wave function of the first excited state, which is ignored by function (19).

It seems interesting to study the dependence of the critical potential and energy gap on the geometrical parameters of the system. The dependences of Φ_{0C} on the gate diameter, calculated using the FEM are shown in Fig. 6. We can see that Φ_{0C} initially decreases with increasing gate diameter, and then, starting from some d, slightly increases. The previously detected initial decrease in Φ_{0C} with increasing gate diameter [2] is associated with expansion of the localization region of the wavefunction near the gate, which results in a decrease in the electron kinetic energy. The increase in Φ_{0C} can be explained taking into account the increase in the degree of overlap of the wavefunctions ψ_G and ψ_D with increasing gate diameter (Fig. 3). It is clear that the growth of Φ_{0C} with increasing z_0 will appear at larger gate diameters.

We note that the dependences shown in Fig. 6 will have a more universal behavior, if the potential difference $\Delta\Phi = \Phi_0 - \Phi(0, z_0)$ (where $\Phi(\rho, z)$ is the distribution function of the potential induced by the gate) is considered as the control parameter, rather than the gate potential. Then, instead of the critical potential, we will consider the critical potential difference $\Delta\Phi_C$. We can see in Fig. 6 that the critical potential difference will be almost independent of the donor position, and formula (11) becomes applicable to any z_0 when Φ_{0C} is replaced with $\Delta\Phi_C$ (it is obvious that Φ_{0C} and $\Delta\Phi_C$ become equal for an infinitely distant donor).

The energy gap between the ground- and first-excited states is associated with overlapping of the gate and donor wavefunctions (ψ_G and ψ_D in representation (19)) at the critical potential Φ_{0C}; therefore, $g_{\min}$ must heavily depend on the donor–gate distance. As shown in Fig. 3, the ψ_G and ψ_D overlap increases even when the gate diameter increases, as a consequence of which $g_{\min}$ also increases (see the inset in Fig. 6). When the gate diameter is much larger than z_0 and the effective Bohr radius, the gate field can be considered uniform, and the dependence of $g_{\min}^{\infty}$ (value of the gap in the case of a uniform external field) on z_0 can be approximated by the expression

$$g_{\min}^{\infty} = a\exp(-\sigma z_0), \qquad (20)$$

where $a = 5.6$ and $\sigma = 0.5$. Formula (20) remains valid even at smaller gate sizes, when the external field already cannot be considered uniform; however, in this case, the parameters a and σ depend on d (see the inset in Fig. 6).

Critical potentials and minimum energy gaps for semiconductors with different effective masses

	a^*, nm	Ry^*, meV	$z_0 = 40$ nm/$d = 40$ nm		$z_0 = 40$ nm/$d = 20$ nm	
			Φ_{0C}, mV	$g_{\min}$, meV	Φ_{0C}, mV	$g_{\min}$, meV
GaAs	10.8	5.15	29.5	6.71	42.1	6.21
$Al_{0.4}Ga_{0.6}As$	6.5	9.37	35.5	2.16	52.6	1.83
Si*	3.16	19.98	52.8	0.081	62.4	0.043
Si**	2.0	31.27	65.8	2.65×10^{-3}	77.7	7.29×10^{-4}

4. EFFECT OF SEMICONDUCTOR PARAMETERS ON THE CONTROL PARAMETERS OF THE STRUCTURE

Expressions (11) and (20) allow us to estimate Φ_{0C} and $g_{\min}$ for various gate diameters and donor–semiconductor surface distances expressed in effective Bohr radii a^*. In this case, the calculated values will be expressed in Ry^*/e and Ry^*. The values obtained for the critical potential are identical to the results of [2], where calculations were performed for relatively small gate diameters. In other works, only the case of the infinite-area gate was studied.

We note that the values of a^* and Ry^* can differ several times for different semiconductors; however, the differences in the critical potentials are not so significant. Let us present the result of some numerical estimations. As an example, we consider four semiconductors: GaAs, $Al_{0.4}Ga_{0.6}As$, and two modifications of "isotropic" Si. We define the first modification (Si*) as a semiconductor with an isotropic mass equal to the transverse mass of Si conduction electrons ($m^* = m_\perp = 0.191m_0$). The second modification (Si**) is chosen from the condition of the equality of Ry^* to the theoretical binding energy of a hydrogenlike donor, $E_{BH} = 31.1$ meV [16]. For both modifications, we take the permittivity equal to that of the Si crystal ($\varepsilon_s = 11.4$). In the former case, we obtain $a^* = 3.16$ nm and $Ry^* = 19.98$ meV; in the latter case, $a^* = 2$ nm, $Ry^* = 31.3$ meV. All four materials have close relative permittivities $\varepsilon_s = 12 \pm 1$, but significantly different effective masses: $0.063m_0$, $0.096m_0$, $0.191m_0$, and $0.3m_0$ for GaAs, $Al_{0.4}Ga_{0.6}As$, Si*, and Si**, respectively [17].

The results of numerical estimations for two values of z_0 are listed in the table. The donor–gate distance was chosen as $z_0 = 40$ nm which corresponds to ~$2a^*$, ~$6a^*$, ~$13a^*$, and ~$20a^*$ for GaAs, $Al_{0.4}Ga_{0.6}As$, Si*, and Si**. At a closer donor–gate distance, determining the critical potential for the case of GaAs is complicated. As follows from the table, at identical gate diameters and donor–interface distances, the energy gap changes most strongly for different semiconductors.

But if we calculate Φ_{0C} for Si* and Si** at $z_0 = 20$ nm (this value of z_0 was proposed for qubits in [1]), we will obtain approximately identical values $\Phi_{0C} \approx (110 \pm 10)$ mV for Si** and Si* at $d = 10$ nm. However, in this case, the values of $g_{\min}$ will differ by a factor of more than 8. Since the actual values of the binding energy of donors in silicon are higher than those theoretically calculated, the values given in the table represent a lower estimate for the critical potential.

The functional dependence of Φ_{0C} on the semiconductor effective mass can be obtained from expression (11) for the case of $d \geqslant 6a^*$. For example, it follows from (11) that the relation

$$\eta = \frac{\Phi_{oC}^{(1)}}{\Phi_{0C}^{(2)}} \approx \left(\frac{m_1^*}{m_2^*}\right)^{1-\tau}, \qquad (21)$$

will be satisfied for semiconductors characterized by effective masses m_1^* and m_2^*, where τ is the quantity defined in Eq. (11) for different boundary conditions. From expression (20), in the case of $d \to \infty$, when the external electric field in the region of wavefunction localization is close to uniform, it follows that

$$g_{\min} \approx bm^* \exp(-k\tilde{z}_0 m^*), \qquad (22)$$

where b and k are certain constants, $\tilde{z}_0$ is the donor–gate distance in SI units. Expression (22) can be the upper boundary for $g_{\min}$ at finite gate diameters (see the inset in Fig. 6).

We note one more application of formula (11): it allows estimation of electric fields near the gate at a gate potential equal to Φ_{0C}. Since the maximum electric field in the structure under study should not exceed the semiconductor breakdown field, formula (11) allows us to estimate the minimum acceptable gate diameters. Neglecting boundary effects, it can be considered that the maximum field is reached at the point with the coordinates $z = \rho = 0$. Then we obtain (in dimensionless units)

$$d > \left(\frac{E_{BD}}{8.44}\right)^{-2/3} \qquad (23)$$

in the case of BC-A and

$$d > \left(\frac{E_{BD}}{35.4}\right)^{-5/9} \qquad (24)$$

in the case of BC-B, where E_{BD} is the semiconductor breakdown field. For example, for Si*, the minimum

acceptable gate diameter will be $d_{\min} \approx 1.5a^*$ and $d_{\min} \approx 3.1a^*$; for Si**, $d_{\min} \approx 2.7a^*$ and $d_{\min} \approx 5.1a^*$ for the cases of BC-A and BC-B, respectively ($E_{BD} = 3 \times 10^7$ V/m). These values are close to the geometrical sizes of control electrodes, proposed for qubits in [1], hence, restrictions to the minimum acceptable sizes of control electrodes should be considered in estimating the feasibility of systems in which the use of the effect of the shuttling of electron wavefunctions between the donor and gate is assumed.

5. CONCLUSIONS

The electric field induced by a disk-shaped metal electrode (gate) on the donor-bound electron wavefunction was numerically simulated. Based on the results of calculations using the finite element method, a trial function describing electronic states in the gate electric field was proposed. Empirical formulas allowing determination of the relation between the critical characteristics of the external field and structure's geometrical parameters were derived. The results of calculations can be used in estimating the possibility of developing nanodevices using control of shallow donor electron states.

APPENDIX

In the case where the region $z < 0$ is filled with insulator, $\hat{V}_G^{(i)}$ is defined, according to [12], as

$$\hat{V}_G^{(A)} = -\frac{2\Phi_0}{\pi}\arctan\left(\frac{d}{2}\sqrt{\frac{2}{\rho^2 + z^2 - \frac{d^2}{4} + \left(\left(\rho^2 + z^2 - \frac{d^2}{4}\right)^2 + d^2z^2\right)^{1/2}}}\right). \quad \text{(A.1)}$$

But if the disk is surrounded by a grounded screen, according to [13], we have

$$\hat{V}_G^{(B)} = -\Phi_0\left(1 - \frac{z}{\pi\sqrt{z^2 + \left(\rho + \frac{d}{2}\right)^2}} \times \left(\frac{a - \frac{d}{2}}{a+\rho}\Pi\left(\frac{\pi}{2}, n_1, k\right) + \frac{a + \frac{d}{2}}{a-\rho}\Pi\left(\frac{\pi}{2}, n_2, k\right)\right)\right). \quad \text{(A.2)}$$

where

$$a = \sqrt{z^2 + \rho^2}, \quad n_1 = -\frac{2\rho}{a+\rho}, \quad n_2 = \frac{2\rho}{a-\rho},$$

$$k^2 = \frac{2d\rho}{z^2 + \left(p + \frac{d}{2}\right)^2}.$$

$\Pi(\pi/2, n, k)$ is a complete elliptic integral of the third kind,

$$\Pi\left(\frac{\pi}{2}, n, k\right) = \int_0^{\frac{\pi}{2}} \frac{d\varphi}{(1 + n\sin^2\varphi)\sqrt{1 - k^2\sin^2\varphi}}.$$

REFERENCES

1. B. E. Kane, Nature (London) **393**, 133 (1998).
2. G. D. J. Smit, S. Rogge, J. Caro, and T. M. Klapwijk, Phys. Rev. B **68**, 193302 (2003).
3. L. M. Kettle et al., Phys. Rev. B **68**, 075317 (2003).
4. D. B. MacMillen and U. Landman, Phys. Rev. B **29**, 4524 (1984).
5. M. J. Calderon, B. Koiller, and S. Das Sarma, Phys. Rev. Lett. **96**, 096802 (2006).
6. M. J. Calderon, B. Koiller, and S. Das Sarma, Phys. Rev. B **75**, 125311 (2007).
7. A. F. Slachmuylders, B. Partoens, F. M. Peeters, and W. Magnus, Appl. Phys. Lett. **92**, 083104 (2008).
8. Y. L. Hao, A. P. Djotyan, A. A. Avetisyan, and F. M. Peeters, Phys. Rev. B **80**, 035329 (2009).
9. V. A. Nikolyuk and I. V. Ignatiev, Semiconductors **41**, 1422 (2007).
10. A. S. Martins, R. B. Capaz, and B. Koiller, Phys. Rev. B **69**, 085320 (2004).
11. http://www.mathworks.com/products/matlab/
12. W. R. Smythe, *Static and Dynamic Electricity*, International Series in Pure and Applied Physics (McGraw-Hill, New York, 1950).
13. N. N. Mirolyubov, M. V. Kostenko, M. L. Levinshtein, and N. N. Tikhodeev, *Methods of Calculating Electrostatic Fields* (Vysshaya Shkola, Moscow, 1963) [in Russian].
14. G. M. Rignanese, J. Phys.: Condens. Matter **17**, R357 (2005).
15. L. D. Landau and E. M. Lifshitz, *Course of Theoretical Physics*, Vol. 3: *Quantum Mechanics: Non-Relativistic Theory* (Nauka, Moscow, 1989, 4th ed.; Pergamon, New York, 1977, 3rd ed.).
16. R. A. Faulkner, Phys. Rev. **184**, 713 (1969).
17. http://www.matprop.ru/

Translated by A. Kazantsev